MRI Tracking of Macrophages Labeled with Glucan Particles Entrapping a Water Insoluble Paramagnetic Gd-Based Agent

Sara Figueiredo[1,4,5], Juan Carlos Cutrin[1,2], Silvia Rizzitelli[1], Elisa De Luca[1], João Nuno Moreira[3,5], Carlos F. G. C. Geraldes[4,5,6], Silvio Aime[1] and Enzo Terreno[1]*

[1] Department of Molecular Biotechnology and Health Sciences and Molecular & Preclinical Imaging Centers, University of Torino, Torino, Italy
[2] ININCA (UBA-CONICET) Argentina
[3] FFUC - Faculty of Pharmacy, University of Coimbra, Coimbra, Portugal
[4] Department of Life Sciences, Faculty of Sciences and Technology, University of Coimbra, Coimbra, Portugal
[5] CNC - Center of Neurosciences and Cell Biology, University of Coimbra, Portugal
[6] Coimbra Chemistry Center, University of Coimbra, Coimbra, Portugal

* Corresponding author:
Prof. Enzo Terreno
Department of Chemistry and Molecular & Preclinical Imaging Centers
Via Nizza 52 – 10126 Torino, Italy.
Phone: +39-011-6706452
Fax: +39-011-6706487
e-mail: enzo.terreno@unito.it

Keywords: MRI, Gadolinium, Paramagnetic MRI agents, Glucan Particles, Cell tracking

Disclosure: This manuscript is the peer-reviewed version of the article Figueiredo S, Cutrin JC, Rizzitelli S, De Luca E, Moreira JN, Geraldes CF, Aime S, Terreno E. MRI tracking of macrophages labeled with glucan particles entrapping a water insoluble paramagnetic Gd-based agent. Mol Imaging Biol. 2013 Jun;15(3):307-15. doi: 10.1007/s11307-012-0603-x.

The final publication is available at
http://link.springer.com/article/10.1007%2Fs11307-012-0603-x

MRI Tracking of Macrophages Labeled with Glucan Particles Entrapping a Water Insoluble Paramagnetic Gd-Based Agent

Sara Figueiredo[1,4,5], Juan Carlos Cutrin[1,2], Silvia Rizzitelli[1], Elisa De Luca[1], João Nuno Moreira[3,5], Carlos F. G. C. Geraldes[4,5,6], Silvio Aime[1] and Enzo Terreno[1]*

[1] Department of Molecular Biotechnology and Health Sciences and Molecular & Preclinical Imaging Centers, University of Torino, Torino, Italy.

[2] ININCA (UBA-CONICET) Argentina.

[3] FFUC - Faculty of Pharmacy, University of Coimbra, Coimbra, Portugal.

[4] Department of Life Sciences, Faculty of Sciences and Technology, University of Coimbra, Coimbra, Portugal

[5] CNC - Center of Neurosciences and Cell Biology, University of Coimbra, Portugal

[6] Coimbra Chemistry Center, University of Coimbra, Coimbra, Portugal

* Corresponding author:

Prof. Enzo Terreno

Department of Chemistry and Molecular & Preclinical Imaging Centers

Via Nizza 52 – 10126 Torino, Italy.

Phone: +39-011-6706452

Fax: +39-011-6706487

e-mail: enzo.terreno@unito.it

Abstract

Purpose: This study aimed at demonstrating the *in vivo* potential of Gd(III)-loaded Glucan Particles (Gd-GPs) as MRI positive agents for labeling and tracking phagocytic cells.

Procedure: GPs were obtained from *Saccharomyces cerevisae* and loaded with the water-insoluble complex Gd-DOTAMA(C_{18})$_2$. The uptake kinetics of Gd-GPs by murine macrophages was studied *in vitro* and the internalization mechanism was assessed by competition assays. *In vivo* performance of Gd-GPs was tested at 7.05 T on a mouse model of acute liver inflammation.

Results: The minimum number of Gd-GPs-labeled J774.A1 macrophages detected *in vitro* by MRI was *ca*. 300 cells /μL of agar, which is the lowest number ever reported for cells labeled with a positive T_1 agent. Intravenous injection of macrophages labeled with Gd-GPs in a mouse model of liver inflammation enabled the MRI visualization of the cellular infiltration in the diseased area.

Conclusions: Gd-GPs represent a promising platform for tracking macrophages by MRI as a T_1 alternative to the golden standard T_2-based iron oxide particles.

Keywords: MRI, Gadolinium, Paramagnetic MRI agents, Glucan Particles, Cell tracking

List of Abbreviations:

Gd-GPs: Gd-loaded Glucan particles

GPs: Glucan particles

Rho-GPs: Rhodamine-loaded Glucan particles

PBS: Phosphate Buffer Saline

ALT: Alanine amino transferase

USPIO: Ultra small superparamagnetic iron oxide particles

SPIO: Superparamagnetic iron oxide particles

MPIO: Micrometer sized iron oxide particles

siRNA: small interfering RNA

Introduction

Tracking immune cells during the progression of a disease is a crucial aspect for getting an in-depth view of their role in several diseases as well as for monitoring the therapeutic outcome. This task requires minimally invasive and sensitive imaging modalities, capable of yielding high-resolution images. For these reasons, Magnetic Resonance Imaging (MRI) is the technique of choice for the observation of cell migration in small-size animals. To date, the most consistent cellular labeling approaches have dealt mostly with iron-oxide nanoparticles (USPIO, SPIO, MPIO) [1-4], but also Gd-based contrast agents have been considered [5-16]. The success of iron-oxide particles is primarily due to the higher sensitivity that is exhibited by these agents. However, a drawback of the superparamagnetic particles can be the negative contrast (based on T_2^* or T_2 relaxation) they generate, which can complicate the detection of cell accumulation in organs with an intrinsic low signal (*e.g.* lungs). Furthermore, the detection of a negative contrast may be confounded with susceptible blood vessels- or bleeding-associated artifacts. Therefore, the use of positive contrast T_1-agents appears to be a promising alternative to overcome these problems, although it requires the entrapment of 10^7–10^8 complexes per cell to achieve a sufficient image contrast [6].

Among the several internalization routes that have been explored aiming at accumulating large quantities of paramagnetic complexes into cells [17], phagocytosis is one of the most relevant for cells with innate phagocytic activity as macrophages, dendritic cells, or neutrophils [18-20]. *In vivo* tracking of immune cells by MRI is still a hot-topic in the biomedical field. Specific applications deal with the monitoring of cell recruitment in acute or chronic inflammation sites, as well as the assessment of their fundamental role/trafficking as a response to exogenous insults.

Herein, we report an innovative methodology that allows a fast internalization of large amounts of Gd complexes into phagocytic cells, upon using Glucan Particles (GPs) as labeling “Trojan horses”.

GPs are hollow and porous particles obtained from the common baker's yeast *Saccharomyces cerevisae* and they are mainly constituted by β-1,3-D-glucan that represents the skeleton of the yeast wall. The particles can be obtained through a complex chemical procedure that depletes yeasts from mannan,

proteins and lipids, thereby producing yeast shells that were first named yeast cell wall particles (YCWPs), and then later glucan particles (GPs) [21]. GPs are almost monodisperse systems with a pseudo-spherical shape of a few microns [22]. The shell pores are rather large and small water-soluble molecules cannot be entrapped, unless the pores are sealed with proper gels [23]. However, it has been envisaged that the particles' core could act as a microreactor where small molecules (hydrophilic, amphiphilic or lipophilic) can be aggregated to form larger systems and, subsequently, stably entrapped G. Ostroff and co-workers elegantly demonstrated the feasibility of entrapping water-soluble bioactive compounds (DNA, siRNA, proteins, drugs), *via* a layer-by-layer technique [24-26], or even nanoparticles [22].

In a recent publication, we have extended the array of chemicals that can be loaded into the particles to amphiphilic compounds of interest in the field of diagnostic imaging [27]. Briefly, the method consisted of swelling the particles in an organic solvent (*e.g.* chloroform) containing the dissolved agent. During this step, the agent equilibrates between the inner core of the particles and the bulk compartment. Then, the particles are pelleted and, after the removal of the organic supernatant, they are suspended in water. The sudden change in solvent polarity promotes the formation of a microemulsion that remains stably entrapped in the GPs core. A very important feature for imaging purposes is that the water-insoluble paramagnetic Gd-DOTAMA-$(C18)_2$-entrapping GPs(Gd-GPs) exhibited an unprecedented relaxivity per particle (3.6×10^8 $mM^{-1}s^{-1}$ at 0.5 T) owing to a very high number of encapsulated paramagnetic centers (1.6×10^7/particle). Therefore, the number of Gd centers conveyed by a single particle is already in the right order of magnitude to allow the MRI contrast detection in a cell population [6].

The presence of β-1,3-D-glucan moieties exposed on the particles surface confers to GPs the ability to recognize β-glucan receptors Dectin-1 and complement receptor 3, which are both expressed by phagocytic cells of the immune system [28-31].

In spite of the enhancement of the labeling efficiency of MRI agents towards macrophages exploiting Dectin-1 receptors has been recently achieved after coating iron oxide nanoparticles with β-glucan [32], no reports of using GPs as carriers of paramagnetic Gd-based agents have yet been published.

On this basis, we report herein the first observations about the use of Gd-GPs as cell labeling agents for the *in vivo* tracking of macrophages by MRI.

Materials and Methods

- Preparation of Glucan particles loaded with water-insoluble imaging agents

β-1,3-D-glucan particles were prepared as described previously [25]. Particles were loaded with Gd-DOTAMA$(C18)_2$ (2 mg/mL, synthesized according to ref. [33]) or rhodamine-DPPE dye (20 μg/mL, Avanti Polar Inc, Alabaster, AL, USA) according to ref. [27].

- Cell Preparation, uptake experiments and MRI analysis

Mouse macrophages (J774A.1), mouse melanoma (B16-F10) and rat hepatoma (HTC) cell lines were obtained from the American Type Culture Collection and cultured in the proper complete media. At 80% confluence, cells were detached and seeded in 10 cm culture dishes at a density of about $1x10^6$ cells. One day after seeding, cells were washed and used for the uptake experiments. Cells were incubated with Gd-labeled GPs (250 μM of Gd-DOTAM-$(C18)_2$ in culture medium) or with Gadoteridol (1 mM in culture medium) (kindly provided by Bracco Imaging SpA), at 37 °C in complete medium. After the proper incubation time, cells were washed three times with PBS, and then detached and transferred into glass capillaries that were placed in an agar phantom for MRI experiments.

- In vitro MRI experiments

MRI-T_1 and T_2-weighted images were performed on a Bruker Avance 300 NMR spectrometer, equipped with a microimaging probe operating at 7.05 T, and on an Aspect M2™ MRI scanner (Netanya, Israel), operating at 1 T. The details of the experiments are reported in the Supplementary material.

- Determination of Gd content in cells

The amount of the cell internalized Gd(III) was determined using inductively coupled plasma mass spectrometry (ICP-MS, Element-2; Thermo-Finnigan, Rodano (MI), Italy) according to the procedure reported in the Supplementary material and the results are presented in Figure 1.

- *Confocal analysis*

Cells were seeded in 26 mm coverslips at a density of about $1x10^5$ cells and 24 h after seeding, the medium was replaced and cells were treated with the proper stimuli. After the incubation with Rho-GPs (0.5 μg/mL of Rhodamine-phospholipid in culture medium), cells were washed and fixed in 4% para-formaldehyde containing 2% sucrose. Hoechst dye (Sigma-Aldrich) was added for nuclear staining. Confocal microscopy analysis was performed using a Leica TCS SP5 (Leica Microsystems Srl.).

- *In vivo MRI studies*

Acute liver damage was induced on 8-week-old male C57BL/6 mice by intraperitoneal injection of CCl_4 (1 mL/kg, 1:1 diluted in olive oil). Prior to the MRI examination, the animals were anesthetized by injecting tiletamine/zolazepam (20 mg/kg Zoletil 100, Virbac, Carros, France), and xylazine (5 mg/kg Rompun, Bayer SpA Milan). Healthy mice injected with labeled cells ($1x10^6$ in 200 μl), or mice with acute liver damage injected with unlabeled cells ($1x10^6$ in 200 μl), were used as control groups (n = 3 for each group).

The details of the MRI scans are reported in the Supplementary material.

The mean MRI signal intensity values were calculated in regions of interest (ROIs) drawn on the liver using T_2-weighted images as anatomical reference. Image pixels with signal equal to or greater than 3 times the standard deviation of the pre-contrast image were colored in red.

Results

Labeling macrophages with Gd-GPs

The labeling performance of Gd-GPs was assessed in three distinct cell lines (J774A.1, B16-F10, and HTC) and compared with the results obtained with Gadoteridol, a commercial, low-molecular weight

T_1-MRI agent already used for cell labeling purposes [6,7,34]. The amount of paramagnetic agent internalized into macrophages, following 16 h of incubation with Gd-labeled β-glucan particles, was markedly higher (*ca*. 250-fold) than the corresponding amounts found with Gadoteridol, whereas non-phagocytic cells did not show a marked difference in the uptake selectivity between the two agents (Figure 1).

The measurement of the longitudinal water protons relaxation rate ($R_1 = 1/T_1$) as a function of the incubation time (Figure S1a and S1b) showed that, besides a superior labeling efficiency, the cellular uptake of Gd-GPs by macrophages occurred on a much faster time scale (*ca*. 6 fold).

The *in vitro* MR imaging performance (in both T_1- and T_2-weighted experiments) of Gd-GPs-labeled cells as a function of the incubation time is reported in Figure S2. It is noteworthy that, differently from T_1-weighted images, the T_2-based contrast is much higher at 7 T than 1 T.

In both T_1- and T_2-weighted images, the MRI contrast generated by the internalized GPs was still observed after 24 hours post labeling (Figure S3), although a slight decrease (especially in T_1 contrast) was detected starting from 6 h post labeling.

Confocal fluorescence microscopy was used to obtain more information about the intracellular trafficking of the particles. After 24 h of incubation with GPs labeled with rhodamine-derivatized phosphatidylethanolamine, the dispersed staining throughout the cell (Figure 2) suggested that the water insoluble fluorescent payload was likely intracellularly released from the GPs.

Cell viability of the cultured macrophages after labeling with Gd-GPs was assessed using the resazurin/resofurin protocol (see Supplementary material). β-glucan particles had no effect on the cell viability with up to 1.5 μg/mL of GPs (Figure S4a). Cell proliferation was also assessed by determining the cell doubling time in the presence or in the absence of the particles using different concentrations of β-glucan. The cell-division rate in the presence of Gd-GPs was found to be almost unaltered, though at the highest concentration used (1.5 mg/mL of β-glucan) the duplication rate decreased (Figure S4b).

Internalization pathway

We then aim at assessing whether in addition to Dectin1 receptor-mediated endocytosis other internalization routes could be involved in the macrophage uptake of GPs. Cells were thus pre-incubated for 2 h with amiloride (inhibitor of macropinocytosis), chloropromazine (inhibitor of clathrin-mediated endocytosis) or filipin (inhibitor of caveolae-mediated endocytosis), followed by incubation with Rho-GPs (see the experimental details in the Supplementary material). Amiloride was found to be the most efficient inhibitor (Figure S5), thereby suggesting that macropinocytosis may play an important role in the internalization process. This observation was confirmed by confocal microscopy experiments that clearly showed an extracellular localization of the particles in the presence of amiloride (Figure S6).

Sensitivity of the MRI detection of Gd-GPs-labeled cells

MRI experiments on Gd-GPs-labeled cells, which were incrementally diluted in low gelling agar, allowed the *in vitro* determination of a number of MRI-detectable macrophages as low as 300 cells/µl of agar (Figure 3a). Furthermore, the number of pixels at which the MRI signal was statistically (99 % level) higher than noise, was superior at 1 Tesla than at 7.05 Tesla (Figure 3b).

In vivo tracking of Gd-GPs-labeled macrophages

The *in vivo* potential use of Gd-GPs to track macrophages by MRI was assessed on a mouse model of liver inflammation based on the intraperitoneal injection of CCl_4 [35].

After the injection of Gd-labeled macrophages, a T_1-weighted signal enhancement was observed in a portion of the liver region, suggesting that the labeled cells successfully reached the inflamed site (Figure 4). Contrarily, the control healthy mice (as well as the mice injected with Gadoteridol, data not shown) did not show any significant increase in the MRI signal.

To validate the MRI results, the same experiment was repeated using Rho-GPs-labeled cells. After 5 h and 24 h post-injection, the liver and spleen were harvested for histo-pathological examination (see the Supplementary material for details). The fluorescence signal detected in the liver (Figure 5, c and d) and spleen (Figure 5, g and h) was clearly higher in the CCl_4-treated mice. The high fluorescence signal

generated by the dye induced a silencing of the background fluorescence of the tissue, as can be seen by comparing the images with the autofluorescence of the healthy liver/spleen (Figure 5, a and e).

The liver sections were also stained with hematoxylin and eosin (H&E) to obtain information on the liver architecture. In contrast to the preserved architecture observed in the livers of the vehicle-treated mice (Figure S7a), the liver from the CCl_4-treated group showed hepatocytes with a moderate degree of fatty change as well as foci of hepatocellular necrosis (Figure S7b), especially at the zone 3 level of the acini. Both pictures were representative images from each experimental group.

Furthermore, the value of alanine transaminase (ALT) in the serum of the CCl_4-treated mice was nearly twice higher than the value present in the control mice (see Supplementary material). Collectively, these results present three of the main hallmarks of the acute CCl_4-induced hepatitis [36].

Discussion

In vivo cell tracking requires imaging modalities with high spatial and temporal resolution and, therefore, MRI is certainly the candidate of choice. However, such a technique has an intrinsic low sensitivity for the detection of imaging probes, and this drawback is continuing to stimulate the demand for improved agents that are able to generate contrast with high efficiency. When the task is to visualize phagocytic cells, the most straightforward approach is to design nano- or micro-sized agents to exploit the natural avidity of such cells towards large particles. Undoubtedly, the gold standard for labeling macrophages for MRI experiments is represented by iron oxide particles. However, the negative contrast based on T_2^*/T_2 relaxation may be not applicable to track cells accumulating in low-signal organs/tissues, and it may additionally lead to false interpretation.

With the purpose of designing innovative positive agents for labeling macrophages, we deemed relevant the exploration of the potential of paramagnetic Gd(III)-loaded GPs that have been recently demonstrated to be very efficient MRI agents [27]. The affinity of GPs loaded with a microemulsion made of the amphiphilic complex Gd-DOTAMA-$(C_{18})_2$ towards murine macrophages (J774A.1) and other two tumor cell lines (melanoma B16.F10 and hepatoma HTC) was first checked *in vitro* and

compared with the performance of Gadoteridol, a clinically approved paramagnetic complex already investigated as a positive labeling agent.

Despite the absence of opsonins and complement in the incubation medium, the overall labeling efficiency of Gd-GPs towards macrophages was much higher than Gadoteridol (*ca*. 250-fold increase in the steady-state uptake and *ca*. 6-fold increase in the uptake kinetic). Regardless of the very different size of the two agents, this observation is justified by the good affinity of GPs towards macrophages. Such experiments also indicated a certain degree of selectivity of GPs over Gadoteridol towards HTC cells, whereas almost no uptake was observed for B16-F10 cells. As HTC cells are known to overexpress several glyco-receptors (glycocalyx, galactoxyl-mannan, scavenger receptors) [37], it is likely that they can mediate the cell internalization of GPs. Conversely, the null uptake by B16-F10 cells is in agreement with reports mentioning that non-phagocytic cells are only able to uptake particles with a size lower than 500 nm [38].

The ability of the labeled cells to generate positive T_1 contrast was monitored over time at two magnetic field strengths, 1 T and 7.05 T. The use of two magnetic fields relies upon the observation that Gd-GPs shows a maximum efficiency of the agent in the range of 0.2-1.5 T [27]. The best T_1 contrast detection was obtained *in vitro* after 18 h of incubation (Figure S1). As the loaded particles can also generate a T_2 contrast [39] (though less efficiently than iron oxide particles), the labeled cells can be also visualized in T_2-weighted images. However, as T_2 contrast increases over the magnetic field, the negative contrast is much better detected at 7.05 T than at 1 T. Furthermore, as a very short T_2 can compromise the detection of T_1-based contrast, 1 T seems to be a promising field for performing MRI experiments on Gd-GPs.

The uptake kinetics for both Gd-GPs and Gadoteridol was monitored measuring the longitudinal relaxation rate (at 1 T and 7.05 T) of macrophages labeled with the MRI agent at different incubation times. The results confirmed the higher enhancement observed at both fields after 18 h of incubation. The uptake of the paramagnetic GPs occurred much faster than Gadoteridol, and the R_1 measured for the

former agent, after 2 h of incubation, was only slightly lower than the value measured after 18 h (Figure S2).

To quantify the sensitivity advantage of labeling macrophages with Gd-GPs, the minimum number of MRI-detectable labeled cells (with positive contrast) was determined *in vitro* and further compared with data reported for Gadoteridol [40]. Figure 3 indicates that 300 cells/μl of agar could be still visible either at 1 T or at 7.05 T, though with a slight contrast loss at the higher field. This result is very promising because it is one order of magnitude more sensitive than the results reported for cells (HTC) labeled with Gadoteridol (5000 cells/μL agar) and slightly lower than the number of Gd complexes internalized by means of the more biologically invasive electroporation (500 cells/μL of agar). To our knowledge, Gd-GPs are the most sensitive cell-labeling T_1-agents reported so far.

Another relevant property for cellular imaging experiments is represented by the time persistence of the contrast, as in some cases (*e.g.* tracking of stem cells) the experiments may last even months. Figure S3 indicates that the contrast generated by macrophages labeled with Gd-GPs is still detectable 24 h post labeling, although with a slight reduction that was more evident for the positive T_1-weighted contrast. In this specific case, as macrophages are typically monitored for no longer than a couple of days after injection, the potential of Gd-GPs is still preserved. The intracellular fate of the imaging agent in the GPs cavity was monitored in J774.A1 cells by confocal fluorescence microscopy upon loading the particles with a fluorescent rhodamine-based amphiphilic dye. The images shown in Figure 2 indicate that 24 h post labeling the fluorescence signal of the internalized agent was more diffused, which could account for the intracellular release of the probe, in spite of the reported stability of GPs at that level [41]. In addition, the observed decrease of the MRI contrast over time is also likely to arise from the probe release (Figure S3). The usefulness of this novel MRI strategy herein presented is further reinforced by its good tolerability at the cell level (Figure S4).

Although the internalization mechanism of GPs in macrophages has been quite thoroughly investigated, a series of competition imaging experiments were carried out to evaluate whether the particles loaded with the imaging agents could be internalized with pathways not mediated by opsonization or Dectin-1

receptors [42] like macropinocytosis, and clathrin- or caveolae-mediated endocytosis. In this respect, the uptake of Rho-GPs was carried out in the presence of the inhibitors amiloride, chloropromazine, and filipin. Interestingly, the results reported in Figures S5 and S6 supported the view that macropinocytosis also contributes to the cellular uptake of the particles. In fact, when co-incubated with amiloride, GPs were primarily bound to the external side of the cell membranes. This finding parallels other published observations in which both phagocytosis and macropinocytosis may concur in the engulfment of particles by macrophages [43-46]. As the Dectin-1-mediated uptake requires an extensive clustering of the receptors on the cell membrane [42], one may speculate that when the particles exceed the number of receptors, the macropinocytosis route can contribute to the uptake process.

As an *in vivo* proof-of-concept, the potential of Gd-GPs for cell tracking MRI studies was tested on a mouse model of CCl_4-induced acute liver inflammation. A recent study from Karlmark and coworkers has demonstrated that within 48 h after the hepatotoxic injury there was a burst of infiltrating macrophages [47]. The validity of the model was checked histologically through standard H&E staining Figure S7 clearly shows the abnormal liver architecture caused by the severe damage induced by the intraperitoneal injection of CCl4. Furthermore, also the ALT enzymatic activity was significantly different between healthy and injured mice (the ratio CCL_4 treated mice/control mice was found equal to 1.8).

The *in vivo* MR imaging experiment consisted of injecting 1 million J774.A1 cells pre-labeled with Gd-GPs into the tail vein of mice. Then, T_{1w} images at 7.05 T were collected 5 and 24 h post-injection. As shown in Figure 4, a statistically significant positive contrast enhancement was detected in the liver of the CCl_4-treated mice already after 5 h post-injection (Figure 5, i and j). Some enhanced spots were also detected for the healthy animals injected with Gd-GPs (Figure 5, k and l). However, such regions appeared rather spotty and inconsistent with the pathology, which involves a wide region of the organ. To confirm this interpretation, the liver and spleen of both CCl_4-treated and healthy mice injected with macrophages labeled with Rho-GPs were explanted and subjected to fluorescence microscopy. The fluorescence detected in the organs of the diseased animals was much higher than the healthy controls,

thus confirming the higher accumulation of the labeled macrophages in the liver and spleen of the CCl_4-treated mice (Figure 5).

Furthermore, the fluorescence signal detected 24 h post injection (as well as the MR signal) was lower than the readout at 5 h. This finding could parallel the *in vitro* observation where the contrast generated by GPs slowly decreased over time.

Taken together, the results from the *in vivo* experiment outline the ability of the GPs-labeled macrophages to migrate to the liver as a response to their recruitment at the inflammation site. As macrophages play a critical role in all phases of host defense, activation of macrophage functions by β-glucans increases immune response. Activation of the macrophages by beta glucans induces several inflammatory reactions as phagocytosis, migration and secretion of cytokines, prostaglandins, nitric oxide or reactive oxygen species [48]. It is suggested that the ability of polysaccharides to activate immune response may also activate T-cell-mediated immunity against malignant cells. Therefore, it is suggested that beta-glucan acts as an effective immuno-modulator and, although beta-glucan inhibits macrophage growth rate at high concentrations, it should not interfere with the regular beta-glucan immuno stimulation [49]

Conclusions

In this work, we demonstrated for the first time that β-glucan microparticles represent a very promising imaging platform for labeling and tracking phagocytic cells. Their micrometer size allows a fast and efficient cellular labeling, thereby improving the detection threshold in tracking experiments. The overall imaging properties of Gd-GPs may be useful to overcome the difficulties often found with iron oxide labels, especially concerning the *in vivo* discrimination between labeled cells and the released imaging reporter. The latter can be released from the injected cells (*ex-vivo* labeling approach) or it can circulate in the blood (*in vivo* labeling approach). As the macrophage recruitment is typically associated with endothelial damage, both labeled macrophages and the imaging agent itself can be present in the lesion, thus leading to an overestimation of the macrophage infiltration, which invariantly requires *ex-*

vivo validation. The size of GPs prevents their extravasation and the contrast arising from the lesion can be uniquely attributed to the infiltrate. In this study, our main goal was to demonstrate the performance of Gd-loaded GPs for the visualization of the macrophage recruitment in a mouse model of acute liver failure, where the use of negative contrast agents can be severely jeopardized by the intrinsic low MR signal observed in this organ. Importantly, the imaging performance of Gd-GPs could be further improved either by increasing the payload of the imaging agent (e.g. adding opsonins and complement in the incubation medium) or by loading the particles with probes with enhanced MRI performance. In addition, GPs could be also used as labeling agents of non-phagocytic cells properly transfected to express Dectin-1 receptors [50].

If imaging cell tracking were to enter in clinical routine, Gd-GPs could find a niche for expressing their potential. For instance, a possible option could be tracking labeled dendritic cells (phagocytic cells able to stimulate a T-cell mediated immune response) that have been thoroughly investigated for the treatment of several diseases including cancer and immunological disorders [51-52].

Acknowledgements

We thank Regione Piemonte (PIIMDMT and nano-IGT projects), Foundation for Science and Technology of Portugal (project PTDC/QUI/70063/2006, contract REDE/1517/ RMN/2005 and grant number SFRH/BD/33187/2007 to SF) and FEDER, for their support. This work was carried out in the framework of the EU COST D38 and TD1004 Actions and EU-FP7 projects ENCITE (grant number 201842) and INMiND (grant number 278850).

References

1. Lu CW, Hung Y, Hsiao JK, Yao M, Chung TH, Lin YS, Wu SH, Hsu SC, Liu HM, Mou CY, Yang CS, Huang DM, Chen YC (2007) Bifunctional magnetic silica nanoparticles for highly efficient human stem cell labeling. Nano Lett 7:149-154.

2. Shapiro EM, Gonzalez-Perez O, Manuel Garcia-Verdugo J, Alvarez-Buylla A, Koretsky AP. (2006) Magnetic resonance imaging of the migration of neuronal precursors generated in the adult rodent brain. Neuroimage 32:1150-1157.

3. Arbab AS, Yocum GT, Kalish H, Jordan EK, Anderson SA, Khakoo AY, Read EJ, Frank JA (2004) Efficient magnetic cell labeling with protamine sulfate complexed to ferumoxides for cellular MRI. Blood 104:1217-1223.

4. Tang KS, Shapiro EM (2011) Enhanced magnetic cell labeling efficiency using -NH2 coated MPIOs. Magn Reson Med 65:1564-1569.

5. Giesel FL, Stroick M, Griebe M, Troster H, von der Lieth CW, Requardt M, Rius M, Essig M, Kauczor HU, Hennerici MG, Fatar M (2006) Gadofluorine uptake in stem cells as a new magnetic resonance imaging tracking method: an in vitro and in vivo study. Invest Radiol 41: 868-873.

6. Geninatti Crich S, Biancone L, Cantaluppi V, Duo D, Esposito G, Russo S, Camussi G, Aime S (2004) Improved route for the visualization of stem cells labeled with a Gd-/Eu-chelate as dual (MRI and fluorescence) agent. Magn Reson Med 51: 938-944.

7. Biancone L, Geninatti Crich S, Cantaluppi V, Romanazzi GM, Russo S, Scalabrino E, Esposito G, Figliolini F, Beltramo S, Perin PC, Segoloni GP, Aime S, Camussi G (2007) Magnetic resonance imaging of gadolinium-labeled pancreatic islets for experimental transplantation. NMR Biomed 20:40-48.

8. Menchise V, Digilio G, Gianolio E, Cittadino E, Catanzaro V, Carrera C, Aime S (2011) In vivo labeling of B16 melanoma tumor xenograft with a thiol-reactive gadolinium based MRI contrast agent. Mol Pharm 8:1750-1756.

9. Hedlund A, Ahrén M, Gustafsson H, Abrikossova N, Warntjes M, Jönsson JI, Uvdal K, Engström M (2011) Gd_2O_3 nanoparticles in hematopoietic cells for MRI contrast enhancement. Int J Nanomedicine 6:3233-3240.

10. Guenoun J, Koning GA, Doeswijk G, Bosman L, Wielopolski PA, Krestin GP, Bernsen MR (2012) Cationic Gd-DTPA Liposomes for Highly Efficient Labeling of Mesenchymal Stem Cells and Cell Tracking With MRI. Cell Transplant 21:191-205.

11. Ribot EJ, Miraux S, Konsman JP, Bouchaud V, Pourtau L, Delville MH, Franconi JM, Thiaudière E, Voisin PJ (2011) In vivo MR tracking of therapeutic microglia to a human glioma model. NMR Biomed 24:1361-1368.

12. Tachibana Y, Enmi J, Mahara A, Iida H, Yamaoka T (2010) Design and characterization of a polymeric MRI contrast agent based on PVA for in vivo living-cell tracking. Contrast Media Mol Imaging 5:309-317.

13. Tran LA, Krishnamurthy R, Muthupillai R, Cabreira-Hansen Mda G, Willerson JT, Perin EC, Wilson LJ (2010) Gadonanotubes as magnetic nanolabels for stem cell detection. Biomaterials 31:9482-9491.

14. Tseng CL, Shih IL, Stobinski L, Lin FH (2010) Gadolinium hexanedione nanoparticles for stem cell labeling and tracking via magnetic resonance imaging. Biomaterials 31:5427-5435.

15. Fizet J, Rivière C, Bridot JL, Charvet N, Louis C, Billotey C, Raccurt M, Morel G, Roux S, Perriat P, Tillement O (2009) Multi-luminescent hybrid gadolinium oxide nanoparticles as potential cell labeling. J Nanosci Nanotechnol 9: 5717-5725.

16. Nolte IS, Gungor S, Erber R, Plaxina E, Scharf J, Misselwitz B, Gerigk L, Przybilla H, Groden C, Brockmann MA (2008) In vitro labeling of glioma cells with gadofluorine M enhances T1 visibility without affecting glioma cell growth or motility. Magn Reson Med 59:1014-1020.

17. New EJ, Parker D, Smith DG, Walton JW (2010) Development of responsive lanthanide probes for cellular applications. Cur Opinion Chem Biol 14: 238-246.

18. Bulte JW, Kraitchman DL (2004) Iron oxide MR contrast agents for molecular and cellular imaging. NMR Biomed 17: 484-499.

19. Ahrens ET, Flores R, Xu H, Morel PA (2005) In vivo imaging platform for tracking immunotherapeutic cells. Nat Biotechnol 23: 983-987.

20. Ottobrini L, Martelli C, Trabattoni DL, Clerici M, Lucignani G (2011) In vivo imaging of immune cell trafficking in cancer. Eur J Nucl Med Mol Imaging 38:949-968.

21. Aouadi M, Tesz GJ, Nicoloro SM, Wang M, Chouinard M, Soto E, Ostroff GR, Czech MP (2009) Orally delivered siRNA targeting macrophage Map4k4 suppresses systemic inflammation. Nature 458:1180-1184.

22. Soto ER, Caras AC, Kut LC, Castle MK, Ostroff GR (2012) Glucan particles for macrophage targeted delivery of nanoparticles. J Drug Deliv 143524.

23. Soto E, Kim YS, Lee J, Kornfeld H, Ostroff G (2010) Glucan Particle Encapsulated Rifampicin for Targeted Delivery to Macrophages. Polymers 2:681-689.

24. Soto ER, Ostroff GR (2008) Characterization of multilayered nanoparticles inside yeast cell wall particles for DNA delivery. Bioconjugate Chem 19:840–848.

25. Tesz GJ, Aouadi M, Prot M, Nicoloro SM, Boutet E, Amano SU, Goller A, Wang M, Guo CA, Salomon WE, Virbasius JV, Baum RA, O'Connor MJ Jr, Soto E, Ostroff GR (2011) Glucan particles for selective delivery of siRNA to phagocytic cells in mice. Biochem J 2011; 436:351–362.

26. Soto E, Ostroff G (2011) Use of beta-1,3-D-glucans for drug delivery applications. In: Biology and Chemistry of Beta Glucan (Volume 1): Beta Glucans-Mechanisms of Action, Vetvicka V, Novak M (Eds) Bentham Press, 82.

27. Figueiredo S, Moreira JN, Geraldes CF, Rizzitelli S, Aime S, Terreno E (2011) Yeast cell wall particles: a promising class of nature-inspired microcarriers for multimodal imaging. Chem Commun 47: 10635-10637.

28. Brown GD, Gordon S (2001) Immune recognition: a new receptor for β-glucans. Nature 413:36–37.

29. Chan GC, Chan WK, Sze DM (2009) The effects of beta-glucan on human immune and cancer cells. J Hematol Oncol 2:25-35.

30. Huang H, Ostroff GR, Lee CK, Wang JP, Specht CA, Levitz SM (2009) Distinct patterns of dendritic cell cytokine release stimulated by fungal beta-glucans and toll-like receptor agonists. Infection and Immunity 77:1774–1781.

31. Huang H, Ostroff GR, Lee CK, Agarwal S, Ram S, Rice PA, Specht CA, Levitz SM (2012) Relative Contributions of Dectin-1 and Complement to Immune Responses to Particulate β-Glucans. The Journal of Immunology 189:312–317.

32. Vu-Quang H, Muthiah M, Lee H.J, Kim Y-K, Rhee JH, Lee J-H, Cho C-S, Choi Y-J, Jeong YY, Park I-K (2012) Immune cell-specific delivery of beta-glucan-coated iron oxide nanoparticles for diagnosing liver metastasis by MR imaging. Carbohydr Polym 87:1159-1168.

33. Anelli PL, Lattuada L, Lorusso V, Schneider M, Tournier H, Uggeri F (2001) Mixed micelles containing lipophilic gadolinium complexes as MRA contrast agents. Magn Reson Mater Phys Biol Med 12:114-120.

34. Gianolio E, Arena F, Strijkers GJ, Nicolay K, Högset A, Aime S (2011) Photochemical activation of endosomal escape of MRI-Gd-agents in tumor cells. Magn Reson Med 65:212-219.

35. Domenicali M, Caraceni P, Giannone F, Baldassarre M, Lucchetti G, Quarta C, Patti C, Catani L, Nanni C, Lemoli RM, Bernardi M (2009) A novel model of CCl4-induced cirrhosis with ascites in the mouse. J Hepatol 51:991-999.

36. Ramachandran R, Kakar S. (2009) Histological patterns in drug-induced liver disease. J Clin Pathol 62:481-492.

37. Becker A, Neumeier R, Heidrich C, Loch N, Hartel S, Reutter W (1986) Cell surface glycoproteins of hepatocytes and hepatoma cells identified by monoclonal antibodies. Biol. Chem. Hoppe-Seyler 367:681-688.

38. Rejman J, Oberle V, Zuhorn IS, Hoekstra D (2004) Size-dependent internalization of particles via the pathways of clathrin- and caveolae-mediated endocytosis. Biochem J 377:159-169.

39. Terreno E, Delli Castelli D, Viale A, Aime S (2010) Challenges for Molecular Magnetic Resonance Imaging. Chem Rev 110:3019–3042.

40. Terreno E, Geninatti Crich S, Belfiore S, Biancone L, Cabella C, Esposito G, Manazza AD, Aime S (2006) Effect of the intracellular localization of a Gd-based imaging probe on the relaxation enhancement of water protons. Magn Reson Med 55: 491-497.

41. Huang H, Ostroff GR, Lee CK, Specht CA, Levitz SM (2011) Robust Stimulation of Humoral and Cellular Immune Responses following Vaccination with Antigen-Loaded β-Glucan Particles. MBio 2:e00164-10.

42. Goodridge HS, Underhill DM, Touret N (2012) Mechanisms of Fc Receptor and Dectin-1 Activation for Phagocytosis. Traffic 13:1062-1071.

43. Schneider B, Schueller C, Utermoehlen O, Haas A (2007) Lipid microdomain-dependent macropinocytosis determines compartmentation of Afipia felis. Traffic 8:226-240.

44. Scherbart AM, Langer J, Bushmelev A, van Berlo D, Haberzettl P, van Schooten F-J, Schmidt AM, Rose CR, Schins RPF, Albrecht C (2011) Contrasting macrophage activation by fine and ultrafine titanium dioxide particles is associated with different uptake mechanisms. Part Fibre Toxicol 8: art.31.

45. Lim JP, Gleeson PA (2011) Macropinocytosis: An endocytic pathway for internalising large gulps. Immunol Cell Biol 89:836-843.

46. Fernando LP, Kandel PK, Yu J, McNeill J, Ackroyd PC, Christensen KA (2010) Mechanism of cellular uptake of highly fluorescent conjugated polymer nanoparticles. Biomacromolecules 11:2675-2682.

47. Karlmark KR, Weiskirchen R, Zimmermann HW, Gassler N, Ginhoux F, Weber C, Merad M, Luedde T, Trautwein C, Tacke, F (2009) Hepatic recruitment of the inflammatory Gr1+ monocyte subset upon liver injury promotes hepatic fibrosis. Hepatology 50:261-274.

48. Tajima T, Murata T, Aritake K, Urade Y, Hirai H, Nakamura M, Ozaki H, Hori M (2008) Lipopolysaccharide induces macrophage migration via prostaglandin D(2) and prostaglandin E(2). J Pharmacol Exp Ther. 326:493-501.

49. Herre J, Marshall AS, Caron E, Edwards AD, Williams DL, Schweighoffer E, Tybulewicz V, Reis e Sousa C, Gordon S, Brown GD (2004) Dectin-1 uses novel mechanisms for yeast phagocytosis in macrophages. Blood 104:4038-4045.

50. Akramiene D, Kondrotas A, Didziapetriene J, Kevelaitis E (2007) Effects of β-glucans on the immune system. Medicina (Kaunas). 43:597-606.

51. Nestle FO, Banchereau J, Hart D (2001) Dendritic cells: on the move from bench to bedside. Nat. Med. 7:761–765.

52. Morel PA, Feili-Hariri M, Coates PT, Thomson AW (2003) Dendritic cells, T cell tolerance and therapy of adverse immune reactions. Clin. Exp. Immunol. 133:1–10.

Captions to the figures

Figure 1. Cellular internalization of Gadoteridol (Gado) and Gd-loaded GPs (GPs) (at 1 mM and 250 μM of Gadoteridol and Gd-DOTAMA-$(C18)_2$, respectively, for 16 h) by macrophages (J774A.1), hepatocarcinoma (HTC) or melanoma (B16-F10) cells. a) Percentage of uptake of Gd(III), b) uptake selectivity between Gd-GPs and Gadoteridol.

Figure 2. a) Confocal microscopy analysis of J774A.1 cells incubated with Rho-GPs (at 0.5 μg/mL of Rhodamine-phospholipid) immediately after the incubation and post 24 h. b) Series of confocal fluorescence pictures taken along the z-axis (z-stack) of J774A.1 cells, 24 h post incubation.

Figure 3. a) T_1w image at 7.05 T and 1 T of J774A.1 incubated with Gd-loaded GPs (at 250 μM of Gd-DOTAMA-$(C18)_2$) and diluted with agar; 1 - unlabeled cells, 2 - 300 cells/μL, 3 - 600 cells/μL, 4 - 1250 cells/μL, 5 - 2500 cells/μL, 6 - 5000 cells/μL; b) representation of the statistically significant enhanced pixels for each cell concentration.

Figure 4. Fat-suppressed T_1-weighted MR images (7.05 T) of two representative mice of the animal group injected with CCl_4 (top row) and the control group (middle row). Both groups were injected with $1x10^6$ J774A.1 cells labeled with Gd-GPs. Column A: images acquired before injecting the labeled cells; columns B-D: post 15 min, post 5 and 24 h, respectively. Bottom row reports the images of column C where the red spots correspond to statistically significant enhanced pixels (see experimental section). Left: CCl_4-treated mouse, right: control mouse.

Figure 5. Fluorescence images of liver and spleen section from healthy and CCl_4-treated mice (a - control liver; b - control liver treated with the labeled cells; c – CCl_4-treated mice, 5 h post injection of the labeled cells; d – CCl_4-treated mice, 24 h post injection of the labeled cells; e - control spleen; f -

control spleen treated with labeled cells; g – CCl_4-treated mice, 5 h post injection of $1x10^6$ Rho-GPs-labeled cells; g – CCl_4-treated mice, 24 h post injection of $1x10^6$ cells Rho-GPs-labeled.

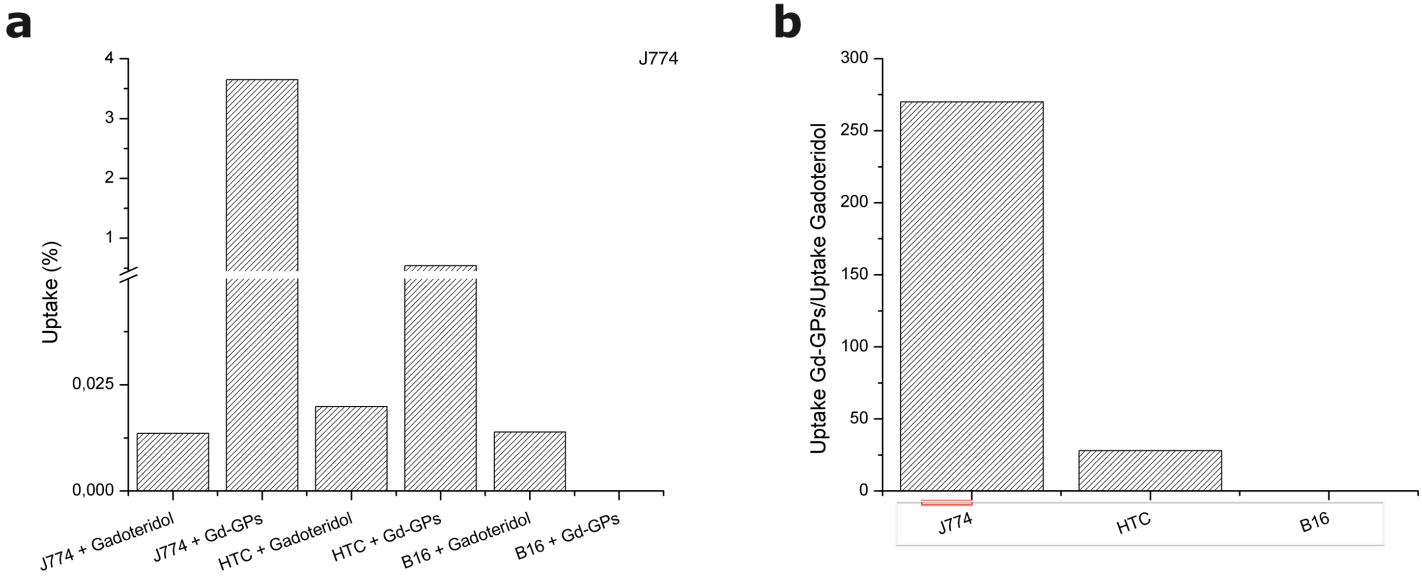
a
J774
Uptake (%)
4
3
2
1
0,025
0,000
J774 + Gadoteridol
J774 + Gd-GPs
HTC + Gadoteridol
HTC + Gd-GPs
B16 + Gadoteridol
B16 + Gd-GPs
b
Uptake Gd-GPs/Uptake Gadoteridol
300
250
200
150
100
50
0
J774
HTC
B16

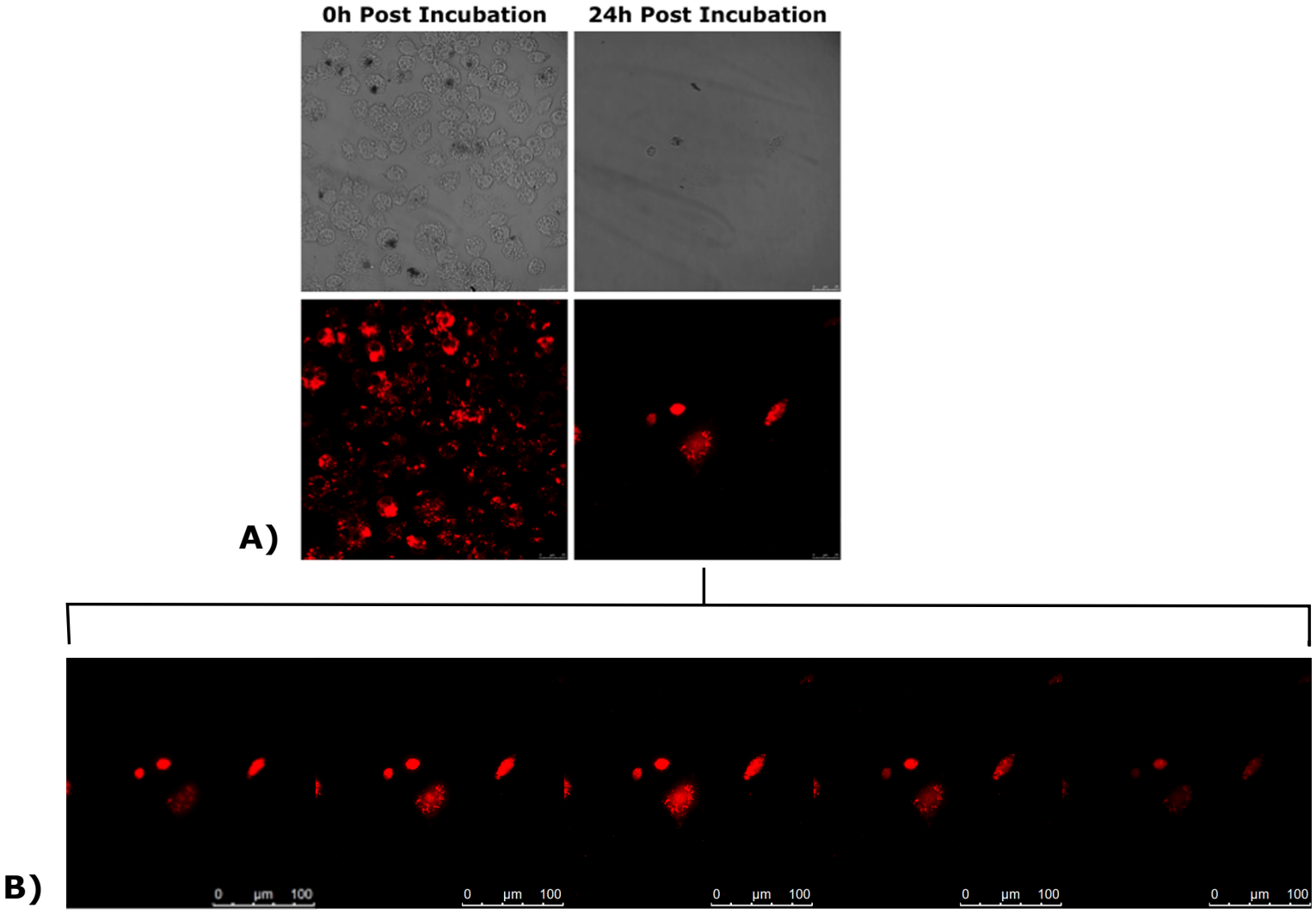
0h Post Incubation
24h Post Incubation
A)
B)
0 µm 100
0 µm 100
0 µm 100
0 µm 100
0 µm 100

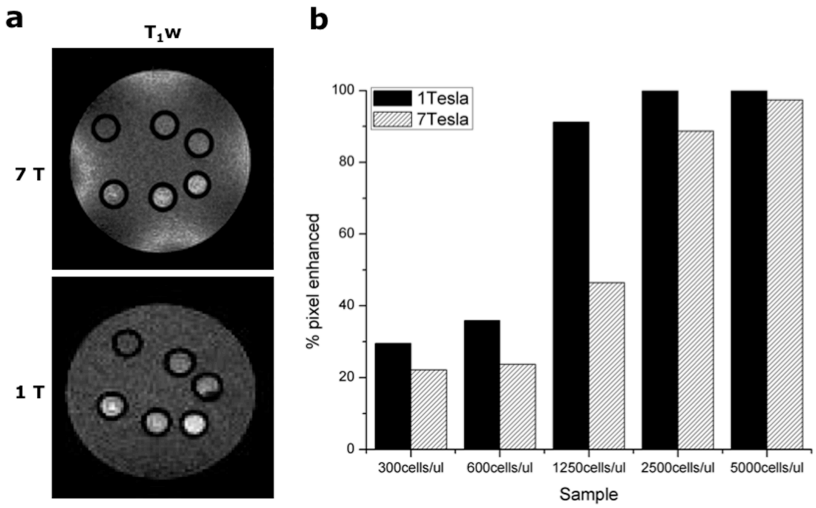
a
T_1w
7 T
1 T
b
1Tesla
7Tesla
% pixel enhanced
100
80
60
40
20
0
300cells/ul
600cells/ul
1250cells/ul
2500cells/ul
5000cells/ul
Sample

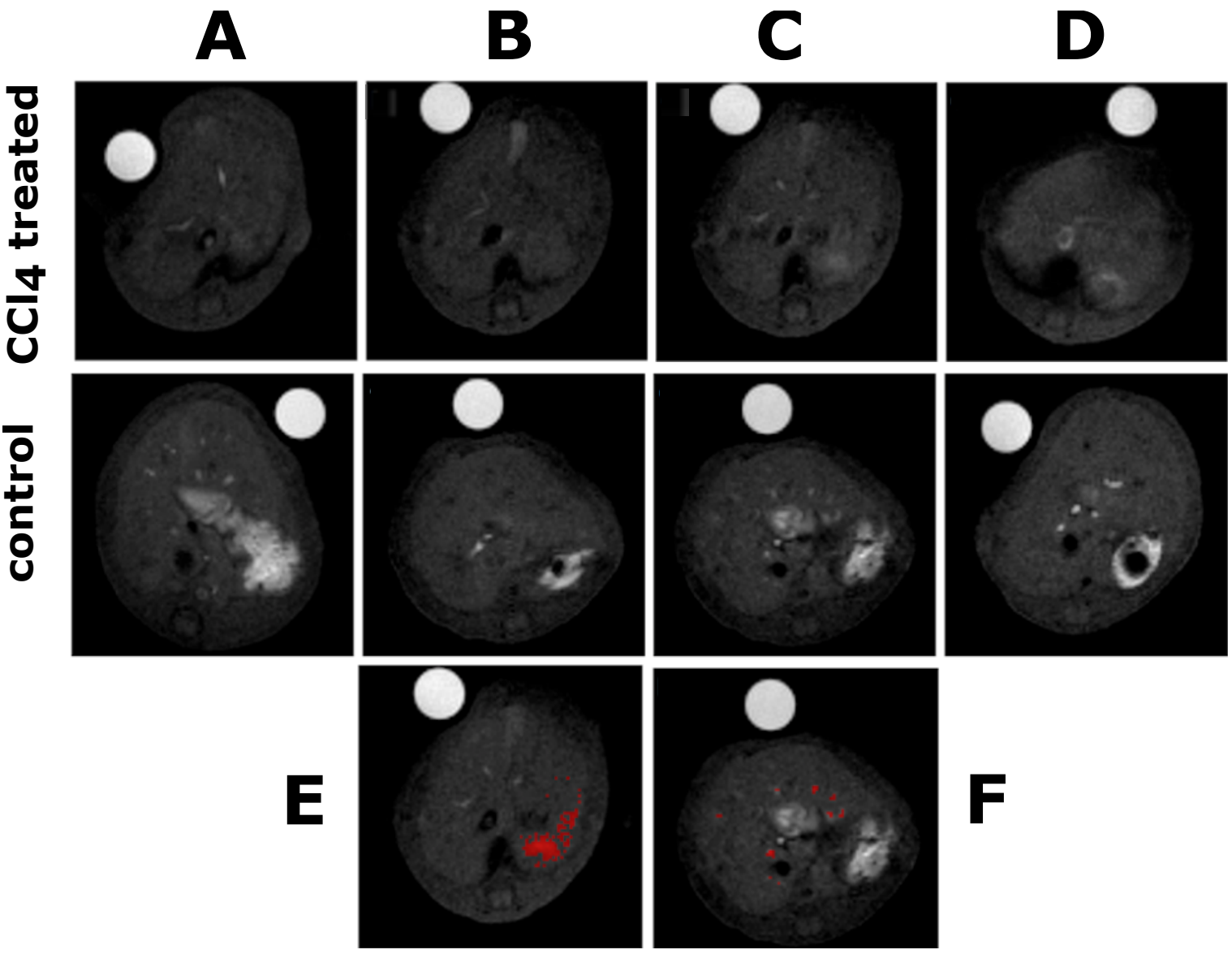
A
B
C
D
CCl4 treated
control
E
F

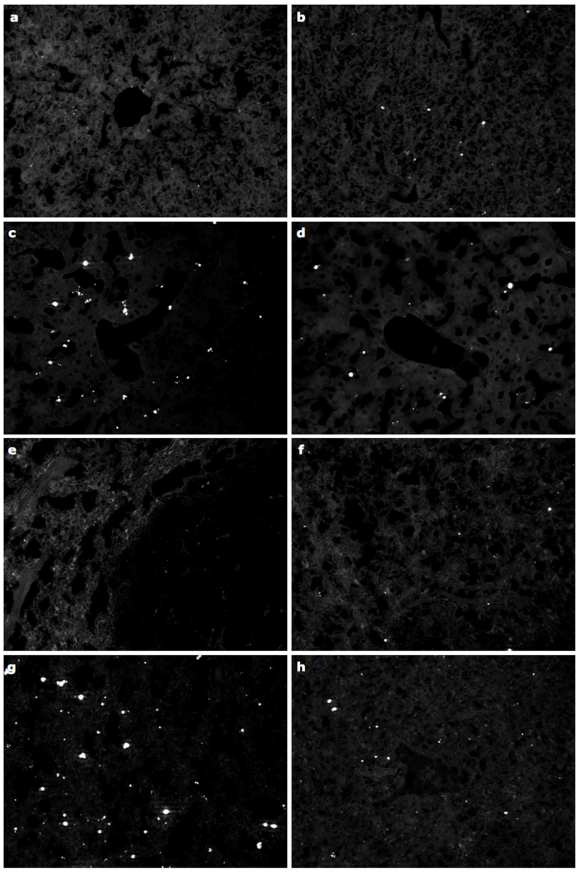
a
b
c
d
e
f
g
h